Pharm Res (2020) 37: 3
https://doi.org/10.1007/s11095-019-2732-2

RESEARCH PAPER

Aerosol Pirfenidone Pharmacokinetics after Inhaled Delivery in Sheep: a Viable Approach to Treating Idiopathic Pulmonary Fibrosis

Lisa M Kaminskas[1] • Cornelia B Landersdorfer[2] • Robert J Bischof[3] • Nathania Leong[3] • Jibriil Ibrahim[3] • Andrew N Davies[3,4] • Stephen Pham[5] • Steven Beck[5] • A. Bruce Montgomery[5] • Mark W Surber[5]

Received: 7 July 2019 / Accepted: 6 November 2019 / Published online: 10 December 2019

ABSTRACT

Purpose Inhaled delivery of pirfenidone to the lungs of patients with idiopathic pulmonary fibrosis holds promise to eliminate oral-observed side effects while enhancing efficacy. This study aimed to comprehensively describe the pulmonary pharmacokinetics of inhaled aerosol pirfenidone in healthy adult sheep. Methods: Pirfenidone concentrations were evaluated in plasma, lung-derived lymph and epithelial lining fluid (ELF) with data subjected to non-compartmental pharmacokinetic analysis. Results: Compartmental pharmacokinetic evaluation indicated that a 49 mg lung-deposited dose delivered an ELF Cmax of 62 ± 23 mg/L, and plasma Cmax of 3.1 ± 1.7 mg/L. Further analysis revealed that plasma pirfenidone reached Tmax faster and at higher concentrations than in lymph. These results suggested inhaled pirfenidone was cleared from the alveolar interstitium via blood faster than the drug could equilibrate between the lung interstitial fluid and lung lymphatics. However, the data also suggested that a 'reservoir' of pirfenidone feeds into lung lymph at later time points (after it has largely been cleared from plasma), prolonging lung lymphatic exposure.

Conclusions This study indicates inhaled pirfenidone efficiently deposits in ELF and is cleared from the lungs by initial absorption into plasma, followed by later equilibrium with lung interstitial and lymph fluid.

KEY WORDS pirfenidone · pharmacokinetics · inhalation · aerosol · lung lymph · sheep · idiopathic pulmonary fibrosis · compartmental modelling

ABBREVIATIONS

AUC	Area under the plasma concentration *vs* time curve
BALF	Bronchoalveolar lavage fluid
Cmax	Maximum concentration
ELF	Epithelial lining fluid
Fabs	Fraction of drug absorbed
IC50	50% inhibitory concentration
Tmax	Time to maximum concentration
IPF	Idiopathic pulmonary fibrosis

INTRODUCTION

Idiopathic pulmonary fibrosis (IPF) is a disease occurring primarily in older adults, characterized by chronic progression and generally poor prognosis (1,2). IPF is a specific form of chronic fibrosing interstitial pneumonia limited to the lung and associated with the pathological pattern of usual interstitial pneumonia. IPF follows a variable clinical course in which periods of relative stability are mixed with episodes of accelerated decline, ultimately resulting in lung transplant, respiratory failure and death.

Much of IPF pathogenesis remains to be understood. However, it is believed that interactions between airway and alveolar epithelial cells with underlying fibroblasts are

✉ Lisa M Kaminskas
L.kaminskas@uq.edu.au

✉ Mark W Surber
msurber@avalynpharma.com

[1] School of Biomedical Sciences, University of Queensland, QLD, St Lucia 4072, Australia

[2] Centre for Medicine Use and Safety, Monash Institute of Pharmaceutical Sciences, Monash University Parkville, VIC 3052, Australia

[3] Allergenix Pty Ltd, Melbourne, VIC 3051, Australia

[4] Biomedicine Discovery Institute, Monash University, Peninsula Campus, Frankston, VIC 3199, Australia

[5] Avalyn Pharma Inc., 701 Pike Street, Suite 1500, Seattle, WA 98101, USA

important for disease initiation and progression (3). Evidence includes recurrent and/or non-resolving epithelial injury stimulating fibroblast accumulation and differentiation into myofibroblasts; accumulated myofibroblasts centralize into fibroblastic foci (regions of excess collagen production); and the close apposition of airway and alveolar epithelial cells with fibroblastic foci. Together, this relationship supports the airway and alveolar surface as the appropriate location for therapeutic drug delivery.

Pirfenidone is a synthetic pyridone compound that inhibits collagen synthesis, down-regulates cytokine production and cytokine-induced response, and blocks fibroblast-to-myofibroblast differentiation (4). Pirfenidone has shown anti-fibrotic and anti-inflammatory activity in a variety of *in vitro* and animal models, and in human IPF. Although oral pirfenidone slows IPF disease progression, substantial side effects often limit its use and effectiveness. More specifically, due to wide biodistribution and low potency, a very large oral dose is required to achieve efficacious lung concentrations (5). Although the US- and EU-approved oral pirfenidone dose (Esbriet®) has been established near the upper safety threshold (801 mg TID; 2403 mg/day), delivered concentrations are below the apparent pirfenidone IC_{50} (approximately 25 μg/ml) (6) and associated blood levels are high and often poorly tolerated. Because associated blood concentrations exist near the upper safety threshold, oral dose escalation for additional efficacy is not possible; a step believed necessary to maximize effect. Complicating matters, dose-absorbing food, first-pass metabolism and safety-driven dose-reduction/stoppage protocols further reduce the lung dose and interrupt required maintenance therapy (5).

To address these shortcomings and maximize its potential, pirfenidone was reformulated for nebulization and inhaled, direct-lung delivery. Preclinical data was then modelled to predict pharmacokinetics in humans after inhaled delivery. These data suggested that a 5 mg nebulized dose will be as efficacious against IPF as an 801 mg oral dose of Esbriet (7). With much less drug required for equivalent efficacy, pirfenidone safety and tolerability are expected to be greatly improved and permit lung-dose escalation for improved efficacy. In support, a recently completed Phase 1 study delivering nebulized pirfenidone to normal volunteers and people with IPF demonstrated that inhalation is safe and well-tolerated (no oral-observed side effects, with limited mild, transient cough), and delivered lung epithelial lining fluid (ELF) concentrations were well-above the pirfenidone IC_{50} with more than 15-fold lower systemic pirfenidone exposure than reported following administration of oral Esbriet (8). With these properties and data supporting efficient peripheral lung deposition in IPF patients, inhalation is predicted to provide a safe and well-tolerated Esbriet alternative or improved-effect stand-alone replacement. As a safe and well-tolerated product, inhalation may also enable pirfenidone's use in desired, but otherwise poorly tolerated add-on combination regimens (e.g., with oral nintedanib; Ofev®).

To better understand pirfenidone's fate following inhalation and the relative benefit of inhaled pirfenidone *versus* Esbriet, we therefore aimed to use sheep (as an appropriate large animal model) to evaluated the kinetics of drug transfer between different compartments in the lung and use this data to predict drug behaviour after inhaled administration in humans using compartmental modelling. In particular ELF, lung derived lymph fluid (as a surrogate measure of pirfenidone concentrations in lung interstitial fluid) and plasma were sampled after nebulization and aerosol administration.

MATERIALS AND METHODS

Materials

Pre-formulated pirfenidone (12.3–14.9 mg/ml, pH 5.6) was supplied by Avalyn Pharma (Seattle, United States) as previously described and was used without further dilution (8). Marcain®, carprofen, xylazine and heparin were purchased from Clifford Hallam Healthcare (VIC, Australia) and saline (0.9% NaCl) was from Baxter (NSW, Australia). Procaine penicillin, cephazolin and Lethabarb were obtained from Virbac (NSW, Australia). Fentanyl transdermal patches were from Janssen Pharmaceuticals Inc. (Beerse, Belgium) and Evans Dye was obtained from Sigma-Aldrich (MO, USA). Isoflurane was from Delvet Pty Ltd. (NSW, Australia). Chlorhexidine was from Livingstone International Healthcare (NSW, Australia). Thiopentone was obtained from Troy Laboratories (NSW, Australia). Sterile polyvinyl catheters (1.5 mm × 2.7 mm) and endotracheal tubes (Portex, 7–8 mm internal diameter) were from Smiths Medical (Aus). Silastic cannula (0.63 mm × 1.19 mm) was obtained from Dow Corning (MI, USA) and was autoclaved sterilised before use.

Animals

Female Merino (*Ovis aries*) cross-bred sheep (approximately 1 year old, 32–40 kg, $n = 12$) were sourced through the Monash Animal Research Platform, Monash University and were acclimatised on site for at least 1 week prior to surgical implantation of cannulas. Animals were treated orally with an anthelminthic drug (1 ml/kg Startec; Zoetis Australia Pty Ltd, NSW, Australia) to eliminate any potential parasites prior to transport to Monash University. After arrival at Monash, bronchoalveolar lavage fluid (BALF) was also collected and examined to confirm the absence of lung parasites in all sheep prior to surgery. Sheep were fasted for 12 h prior to surgery and provided ad *libitum* access to food and water at all other

times. Sheep were housed in metabolic cages after surgery and for the remainder of the study to allow sample collection.

Sheep were housed under ambient conditions (20–22°C) and were maintained on a 12 h light/dark cycle. All animal experimentation was approved by the Monash University Animal Ethics Committee (MMCA-2017-11) and conducted in accordance with the Australian Code of Practice for the Care and Use of Animals for Scientific Purposes.

Surgical Cannulation of the Carotid Artery, Jugular Vein and Efferent Caudal Mediastinal Lymph Duct

Sheep were given intramuscular (IM) xylazine (0.2 mg/kg) to provide pre-surgical sedation, then anaesthetized via intravenous (IV) administration of thiopentone (20 mg/kg). Sheep were immediately intubated with a cuffed endotracheal tube and connected to a mechanical ventilator to maintain anaesthesia with isoflurane (2.5% in oxygen) during surgery. Sheep were then given subcutaneous (SC) carprofen (4 mg/kg), 400 mg IM procaine penicillin and 1 g IV cephazolin to limit inflammation and prevent infection. Marcain (2–5 ml per incision site) was injected SC and into the 5th intercostal space to provide local anaesthesia and nerve block at the incision sites. Fentanyl patches (75 μg) were applied to the skin under the right leg to provide post-surgical analgesia during recovery and withdrawn 24 h before the first pirfenidone dose. Catheters were inserted into the right jugular vein and carotid artery to allow IV dosing and serial blood sampling, respectively. Cannula patency was maintained by flushing with heparinized saline (10 U/ml) daily and after blood sample collection. The efferent caudal mediastinal lymph duct (CMLD), which drains from the caudal mediastinal lymph node (CMLN) into the thoracic lymph duct, was then cannulated with 1 mm silastic tubing via thoracotomy as previously described (9,10). This surgery is associated with an approximately 50% success rate, with approximately 40% of sheep having CMLD anatomy that is not easily cannulated and another 10% losing patency within 24 h after surgery. The silastic cannula was exteriorized through an incision in the chest to allow continuous collection of lung-derived lymph into a sterile EDTA tube or cell culture flask that were held in place with thin elastic netting. Prior to first pirfenidone dose, surgical recovery was allowed for 2–3 days in individual metabolism cages with rubber floor matting.

Pirfenidone Administration and Sample Collection

Each sheep received four pirfenidone doses (as defined in Table I and in the order presented). Each dose was followed by a 24 h sample collection period and an additional 24 h washout prior to the next dose. Dose groups included: 1) Inhaled dose with blood and lymph collection (to evaluate plasma and lymphatic pharmacokinetics); 2) IV dose with blood collection (to calculate pulmonary bioavailability); 3) inhaled dose with lung function testing, blood and bronchoalveolar lavage fluid collection (to determine maximum pirfenidone ELF concentrations and clearance kinetics); and 4) IV dose with lung function testing. Sampling times are described in Table I.

Inhaled administration and BALF collection were facilitated by moving sheep into a specialised body sheath fitted with a harness to restrict head and neck movement. Aerosol delivery to the lungs was performed through a cuffed endotracheal tube that was inserted into the trachea via the nasal passage and attached to a dual phase respirator (Harvard Apparatus, MA, USA) to control the rate and depth of breathing motions (20 breaths per minute, 50% inspiration). The pirfenidone solution (8 ml, containing 119 mg drug) was aerosolised using an PARI eFlow® Inline vibrating mesh nebulizer (Gräfelfing, Germany). The PARI Inline device produced a pirfenidone aerosol with 3.44 um mass median diameter particles and 1.57 geometric standard deviation and delivered the 8 ml dose

Table I Samples Collected and Sample Collection Times for Each Dose Group

Group	Dose	Sample collection times
1	Inhaled dose 1	Blood and lymph samples:
		Collected pre-dose, and at 5, 10, 15, 20, 30, 45, 60, 70, 80, 90 min and 2, 2.5, 3, 4, 6, 8, 12 and 24 h after the start of dosing
2	IV dose 1	Blood samples:
		Collected pre-dose and at 5, 10, 20, 30, 40, 50, 60, 70, 80, 90 min and 2, 2.5, 3, 4, 6, 7, 12 and 24 h after the start of dosing
3	Inhaled dose 2	BALF and blood samples:
		Collected pre-dose and at 5, 15, 30 min after the completion of dosing
		Lung function testing:
		Pre dose and within 10 mins of dose completion
4	IV dose 2	Lung function testing alone:
		Pre dose and within 10 mins of dose completion

over 16 ± 3 min (mean ± sd). Based upon pulmonary pharmacokinetic data of nebulized, inhaled pirfenidone obtained in normal healthy volunteers and in IPF patients, which included determinations of the 'lung delivered dose' (reference 8 and unpublished preliminary trial data), the lung delivered dose in sheep was estimated to be 41.5% of the nominal (119 mg) dose, or 49 mg delivered to the lungs of each sheep. This value was also consistent with lung delivery simulations undertaken by PARI using the same respiratory circuit and parameters used in this study. Blood samples (5 ml) and total draining lung lymph were collected into EDTA-coated tubes at the times described in Table I. Samples were collected from the start of dosing. To calculate percent dose recovered, the volume of lung lymph collected at each time point was recorded. Collected blood and lymph samples were stored on ice until processing. To remove cells, samples were centrifuged at 4°C for 10 min. Supernatant aliquots were frozen at −20°C until analysis.

Because sheep gastrointestinal anatomy does not represent humans, to emulate plasma levels following oral administration, pirfenidone was infused intravenously. IV dosing was performed via the jugular vein cannula (420 mg in 38 mL infused over 58 min) while sheep remained in their metabolism cage. Residual dose in the catheter was infused with 5 ml saline over the last 2 min. This IV dose was predicted to provide plasma concentrations roughly consistent with those obtained after oral Esbriet dosing in humans.

Because the BALF procedure and animal stress during lung function testing may alter pirfenidone plasma and lymph pharmacokinetics, BALF collection and lung function testing were excluded from groups 1 and 2, and only performed in groups 3 and 4. Briefly, BALF was sampled from different lung regions using a catheter inserted down the bronchoscope biopsy port at the nominal times described above in Table I. Actual collection times were recorded for compartmental modelling. Warm saline (20 ml) was slowly introduced into the lungs and immediately withdrawn. Approximately 5–15 ml was recovered at each time point. Blood samples were simultaneously collected with BALF to allow back calculation of ELF dilution (using the urea correction method (11)) and plasma pirfenidone quantification. To remove cells, recovered BALF was centrifuged at 4°C for 10 min (5000 x g) and 500 ul aliquots frozen for later pirfenidone and urea analysis.

Evaluation of Lung Function

Lung function measures were recorded in awake, consciously breathing sheep. Analysis was performed using a fiber-optic bronchoscope and respiratory monitoring set-up (9,12). Lung measures were recorded during normal breathing over a 10-min period prior to and following the second inhaled and IV doses (Table I; Groups 3 and 4). Lung parameters (transpulmonary pressures, dynamic compliance, flow rates and lung volumes) were derived from averaged measures of five epochs of five breaths. The transpulmonary pressure was related to lung and chest wall compliance and is considered an index of effort needed to maintain adequate ventilation.

Quantification of Pirfenidone in Biological Samples

Pirfenidone concentrations were determined using a qualified high-performance liquid chromatography–mass spectrometry/mass spectrometry method (method MN17116 validated for other species matrix and qualified for sheep plasma, lymph and BALF; linear quantifiable range 5–5000 mg/ml; MicroConstants, Inc., San Diego, CA; commercial in confidence). The pirfenidone ELF concentration was determined using the urea correction method (11).

Non-compartmental and Compartmental Pharmacokinetic Analysis

Non-compartmental plasma pharmacokinetic parameters were initially evaluated to compare directly to lymphatic pharmacokinetic parameters as previously described (9). Initial (alpha) and terminal (beta) plasma and lymph (k) elimination rate constants were obtained by linear regression analysis of the data points determining the initial or terminal slope, respectively. The individual areas under the plasma concentration-time profiles (AUC) were calculated using the linear trapezoid method and extrapolated to infinity by dividing the last concentration measured by k. Observed maximum plasma concentrations (Cmax) and time to Cmax (Tmax) were read directly from the data. Pulmonary bioavailability was calculated by dividing inhaled (AUC/dose) by IV (AUC/dose). The cumulative proportion of the dose recovered in lymph was calculated by dividing the mass of pirfenidone recovered in collected lymph at each time by dose × 100 and adding this value to values calculated at earlier time points until lymph concentrations dropped below the limit of quantification.

Compartmental population pharmacokinetic modelling of pirfenidone after inhaled dosing was undertaken via nonlinear mixed-effects modelling. This was performed using the S-ADAPT platform (version 1.57) with the Monte Carlo parametric expectation maximization algorithm (importance sampling, pmethod = 4). The SADAPT-TRAN program was used for pre- and post-processing (13,14).

Initially, pirfenidone plasma concentrations from all sheep following inhaled and IV administration were fitted simultaneously to characterise the systemic disposition of the drug

and to exclude potential of 'flip-flop' kinetics after inhaled dosing. Models containing one, two and three disposition compartments were evaluated. Pirfenidone concentrations in ELF and plasma from all sheep after inhaled dosing were then modelled simultaneously. Models including one or two disposition compartments for ELF, and two disposition compartments for plasma and peripheral tissues were evaluated and the best performing model was carried forward as the basis for the next step. Models incorporating one and two first order processes to describe distribution of pirfenidone from the lungs into the systemic circulation were tested. The best performing model was chosen to be taken forward. Subsequently, pirfenidone concentrations in ELF, plasma as well as lymph from all sheep were modelled simultaneously. Models including distribution of pirfenidone between plasma and lymph, ELF and lymph, and both, were evaluated. Models incorporating processes that described distribution of the drug between peripheral compartments and lymph, elimination from lymph, and distribution from the lungs to a theoretical 'cell compartment' and following that to lymph, were also tested.

A log-normal distribution was used to describe the inter-individual variability of the pharmacokinetic parameters. Models with partial and full covariance matrices were evaluated. The residual unexplained variabilities for pirfenidone in ELF, plasma and lymph were described by combined proportional and additive error models. For model evaluation, plots of observed *versus* individual-fitted and observed *versus* population-fitted pirfenidone concentrations, visual predictive checks and the objective function in S-ADAPT ($-1 \cdot$ log-likelihood) were utilized. The log-likelihood ratio test was used for comparison of nested models and the Akaike criterion for non-nested models.

The final model included one compartment for pirfenidone in ELF, two compartments in plasma and peripheral tissues and one compartment in lymph. In addition, a single compartment acting as a pirfenidone 'reservoir' in distribution equilibrium with drug in lymph was required to adequately describe the observed slower decline of pirfenidone concentrations in lymph compared to plasma. Inclusion of further complexities did not improve the model's goodness of fit to the data. All initial conditions were zero.

The amount of pirfenidone in the ELF compartment (A_{ALF}) was modelled as:

$$\frac{dA_{ELF}}{dt} = Input - CL_{D1,ELF}.C_{ELF} + CL_{D,ELF}.C_1 \quad (1)$$

where Input represents the inhaled administration of pirfenidone, $CL_{D,ELF}$ describes the distribution of pirfenidone between the ELF and the central (plasma) compartment, C_{ELF} is the pirfenidone concentration in ELF, and C_1 the concentration in plasma.

The amount of pirfenidone in the central compartment (A_1) was modelled as

$$\frac{dA_1}{dt} = -\left(CL + CL_{D,ELF} + CL_{D2} + CL_{D,ly}\right).C_1 + CL_{D,ELF}.C_{ELF} + CL_{D2}.C_2 + CL_{D,ly}.C_{ly} \quad (2)$$

where CL is elimination clearance of pirfenidone, CL_{D2} describes the distribution of pirfenidone between the central and the peripheral compartment, $CL_{D,ly}$ the distribution of pirfenidone between the central and the lymph compartment, C_2 the pirfenidone concentration in the peripheral compartment and C_{ly} the pirfenidone concentration in the lymph compartment.

The amount of pirfenidone in the peripheral compartment (A_2) was modelled as:

$$\frac{dA_2}{dt} = -CL_{D2}.C_2 + CL_{D2}.C_1 \quad (3)$$

The amount of pirfenidone in the lymph compartment (A_{ly}) was modelled as:

$$\frac{dA_{ly}}{dt} = -\left(CL_{D,ly} + CL_{D3}\right).C_{ly} + CL_{D,ly}.C_1 + CL_{D3}.C_3 \quad (4)$$

where CL_{D3} describes the distribution of pirfenidone between the lymph compartment and the reservoir compartment, and C_3 the pirfenidone concentration in the reservoir compartment.

The amount of pirfenidone in the reservoir compartment (A_3) was modelled as:

$$\frac{dA_3}{dt} = -CL_{D3}.C_3 + CL_{D3}.C_{ly} \quad (5)$$

Statistical comparison of pre-dose *versus* post-dose lung function

Lung function parameters obtained before and after inhaled or IV dosing, were compared via a paired Student's T test. Significance was determined at a level of $p < 0.05$.

RESULTS

Lung Function before and after IV and Inhaled Pirfenidone Administration

Lung function was assessed in five animals before (pre-) and after (post-) the IV and inhaled pirfenidone administration. There were no significant changes observed in

transpulmonary pressures (airway resistance), dynamic compliance, ventilation or tidal volumes in response to either the IV or inhaled pirfenidone administration (Fig. 1).

Pulmonary Pirfenidone Pharmacokinetics

Using non-compartmental analysis, pirfenidone pulmonary bioavailability was essentially complete at 102 ± 18% (Table II). Using a 49 mg inhaled lung delivered dose and setting the population mean bioavailability to 100% (based on the non-compartmental F_{abs}), compartmental results estimated the inter-individual variability in bioavailability to be 29% and 4% for groups 1 and 3, respectively (Table III). The lower value for estimated inter-individual variability in bioavailability between the sheep in group 3 was most likely due to the sparser sampling times (three observations per sheep). Therefore, the estimated inter-individual variability in bioavailability between the sheep in group 1 is most likely more reflective of the actual variability.

Intravenous infusion of 420 mg pirfenidone over 1 h gave an apparent plasma C_{max} of approximately 8000 ng/ml (Fig. 2a), consistent with Cmax values in humans delivered an 801 mg oral dose(6). The drug was cleared from plasma with an elimination half-life of 0.9 ± 0.03 h (mean ± SEM).

Table II Non-Compartmental Pirfenidone Pharmacokinetic Parameters After Inhaled Administration to Sheep. Data Represent Mean ± SEM ($n = 5$)

Parameter	Units	Plasma	Lymph
AUC	μg.h/ml	1.56 ± 0.38	1.32 ± 0.09
F_{abs}	–	1.02 ± 0.18	–
K_{alpha}	h^{-1}	3.113 ± 0.564	–
K_{beta}	h^{-1}	1.006 ± 0.112	0.262 ± 0.053
Alpha T½	h	0.25 ± 0.04	–
Beta T½	h	0.73 ± 0.09	3.0 ± 0.5
C_{max}	ng/ml	3508 ± 958	1764 ± 72
T_{max}	h	0.25 ± 0.05	0.33 ± 0.00

The apparent plasma Cmax of pirfenidone after aerosol administration of around 3500 ng/ml was non-compartmentally identified at a Tmax of approximately 0.25 h (Table II, Fig. 2b), consistent with the average aerosol dosing time. From this point, pirfenidone plasma concentrations rapidly declined and followed 2-compartment elimination kinetics which was used to inform the compartmental modelling. Cmax and Tmax in plasma from compartmental modelling were very similar to the results from non-compartmental analysis (Table III). Results from compartmental modelling support a rapid absorption

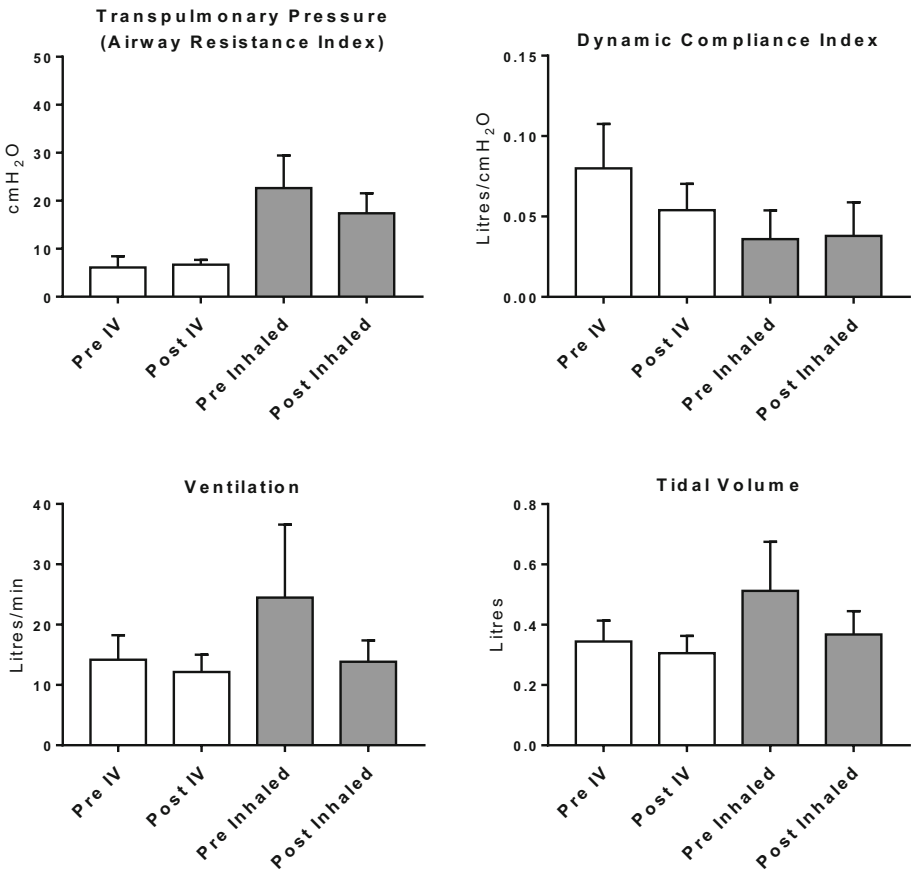

Fig. 1 Lung function assessment in sheep pre- and post- IV and inhaled pirfenidone administration. Data expressed as mean ± SEM (n = 5).

Table III Population Parameter Estimates and Their Inter-individual Variability (IIV) for Pirfenidone in ELF, Plasma and Lymph

Parameter [a]	Symbol	Unit	Estimate	IIV %CV
ELF compartment				
Apparent volume of ELF compartment	V_{ELF}	L	0.431	33.8
Distribution clearance between ELF and central compartments	$CL_{D,ELF}$	L/h	2.61	5.08
Proportional residual variability	CV_{ELF}	%	65.8	–
Additive residual variability	SD_{ELF}	mg/L	0.131	–
Central and peripheral compartments				
Total body clearance	CL	L/h	33.6	27.7
Volume of central compartment	V_1	L	0.302	36.0
Volume of peripheral compartment	V_2	L	7.85	6.13
Distribution clearance between central and peripheral compartments	CL_{D2}	L/h	21.4	28.3
Bioavailability in inhaled group 1	F_1	%	100 [b]	28.6
Bioavailability in inhaled group 3	F_2	%	100 [b]	4.05
Proportional residual variability	CV_{CP}	%	24.0	–
Additive residual variability	SD_{CP}	mg/L	0.00194	–
Lymph and reservoir compartments				
Volume of lymph compartment	V_{ly}	L	0.560	8.86
Distribution clearance between central and lymph compartments	$CL_{D,ly}$	L/h	8.60	123
Volume of reservoir compartment	V_3	L	13.4	165
Distribution clearance between lymph and reservoir compartments	CL_{D3}	L/h	3.50	9.55
Proportional residual variability	CV_{ly}	%	11.0	–
Additive residual variability	SD_{ly}	mg/L	0.0122	–

[a] Reported parameters are apparent clearances and apparent (not physiological) volumes of distribution because pirfenidone was administered through the lungs, assuming 100% bioavailability based on non-compartmental analysis. Detailed distribution kinetics of pirfenidone in the lungs are unknown

[b] Fixed to 100% based on non-compartmental results

of pirfenidone into plasma following inhaled aerosol administration.

Only approximately 0.01% of the inhaled pirfenidone dose was recovered in total lung lymph collected over the 24 h sampling period (Fig. 3a), and accumulation in lymph appeared to cease prior to 2 h, consistent with the rapid decline in plasma concentrations (Fig. 2b). Compared to plasma, the lung lymph pirfenidone Cmax (1800 ng/ml) was approximately two-fold lower, Tmax (0.33 h) slightly delayed (Table II, Fig. 2a), and terminal elimination half-life (3 h) considerably longer. As a result, the lymph AUC was similar to the plasma AUC (Table II). Lymph concentrations were well

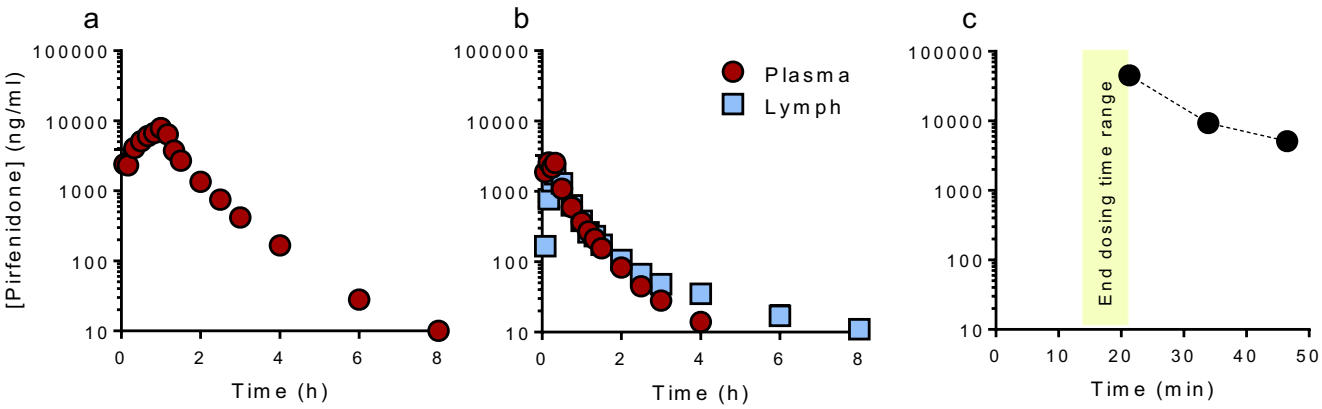

Fig. 2 Pirfenidone concentration *vs* time profiles in plasma, lung lymph and ELF. **(a)** Plasma concentrations after IV infusion of 420 mg pirfenidone over 1 h (approx. 12 mg/kg dose). **(b)** Plasma and lymph concentrations after a 49 mg inhaled pirfenidone dose over approx. 16 min (approx. 1.4 mg/kg). **(c)** ELF concentrations after a 49 mg inhaled pirfenidone dose over approx. 17 min (approx. 1.5 mg/kg). Time points represent the time after dose initiation. Data represents mean ± SEM ($n = 5$).

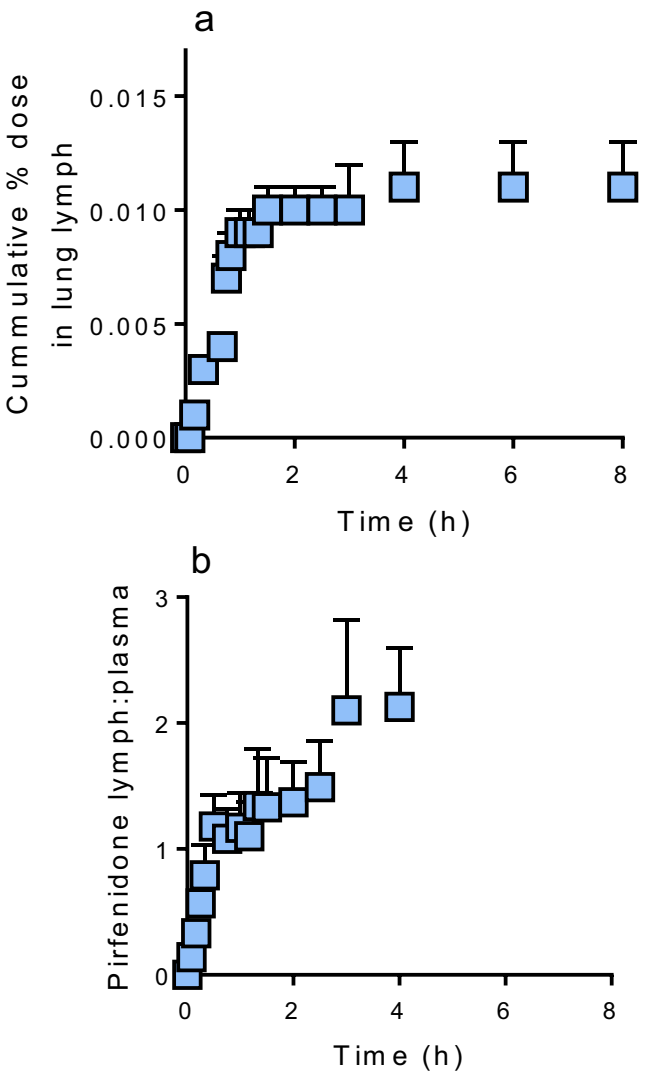

Fig. 3 **(a)** Cumulative percent of inhaled pirfenidone recovered in lung lymph. **(b)** Lymph:plasma pirfenidone ratio. Time initiates with start of dosing. Data represents mean ± SEM (n = 5)

described by the compartmental model (Table III) incorporating first order distribution of pirfenidone from plasma to lymph. Inclusion of a 'reservoir compartment' from and to which pirfenidone in plasma appeared to distribute, was required to adequately describe the longer terminal half-life of pirfenidone in lymph compared to plasma and the increase over time in the lymph:-plasma concentration ratios (Fig. 3b). Specifically, lymph:plasma ratios and trends showed a gradual increase in lymph:plasma from 0 to 1 over the dosing period (consistent with the gradual transfer of drug from plasma into interstitial fluid and lymph), followed by accumulation of pirfenidone in interstitial fluid (reflected in lymph:plasma of >1).

A high degree of variability was noted in the pirfenidone concentrations quantified in ELF, especially at the early time points (see supporting information). The first BALF sample was collected approximately 5 min after the end of nebulization. Earlier sampling times were not possible. The ELF concentrations measured at the three time points in each sheep indicated high initial sample concentrations, followed by a rapid decline in ELF pirfenidone due to fast absorption into the systemic circulation. This was supported by the plasma concentration time profiles following inhaled aerosol administration. This data enabled the model to predict the Cmax values shown in Fig. 4, collectively for sheep in aerosol group 1 (frequent plasma sampling) and group 3 (BALF sampled, but few plasma samples). Concentrations in ELF following nebulized administration were well described by the compartmental model that incorporated complete pirfenidone absorption from ELF into plasma, which was fitted by a first order process (Table III and supporting information Fig. S1). The AUC values for pirfenidone in ELF reported in Fig. 4 are based on integration of the individual model fitted (individual predicted) plasma concentration time curves (supporting information). The model predicted Cmax and AUC values are based on the model assumptions of a zero order (constant rate) input of pirfenidone into ELF during inhaled administration and a first order decline of drug concentrations in ELF due to absorption into the central circulation. The final model demonstrated highly sufficient predictive performance for pirfenidone in plasma, ELF and lymph, as evidenced by visual predictive checks (supporting information, Fig. S1). Inclusion of further complexities into the model did not substantially improve model performance. The elimination half-life from ELF was 7 min based on the population mean parameter estimates and the estimated individual half-lives in ELF ranged from 5 to 10 min.

Further predictive modelling was then performed on 1000 virtual simulated sheep to predict ELF exposure over an 11 min aerosol delivery time (see supporting information). This approach predicted median ELF Cmax concentrations of up to 103 mg/L.

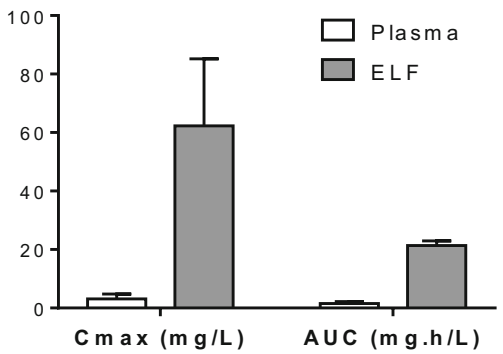

Fig. 4 Model predicted AUC and Cmax values in ELF based on individual fitted curves for sheep in aerosol groups 1 and 2. Data represent mean ± SD (*n* = 10 across 5 sheep)

DISCUSSION

Inhaled pirfenidone has the demonstrated potential to significantly improve IPF treatment and eliminate side effects from oral dosing (7,8). A recent human clinical trial suggested inhaled administration delivers pirfenidone ELF concentrations that are both well above the drug's apparent IC_{50} and that possible after oral dosing. However, due the invasive nature of lavage sampling and the need for repeat collection, detailed human ELF concentration curves and information about possible interstitial drug concentrations are not possible. Therefore, the purpose of this study was to use the large animal sheep model to establish the more detailed pharmacokinetic behaviour of pirfenidone following inhalation, and in doing so predict possible patterns of drug transfer and lung/systemic concentrations in humans and overall benefit of the inhaled *versus* oral dosing approach. In addition, we aimed to obtain data on the airway responsiveness of the lungs to the inhaled delivery of pirfenidone by undertaking lung function tests in sheep before and after dosing. An additional advantage of using the sheep model is that, unlike other species, they have reactive airways allowing their use in asthma studies. To this end, this study incorporated measures of airway pressures that would indicate development of bronchospasm with aerosolized pirfenidone.

Sheep plasma, lung-derived lymph and ELF concentrations were compared after an estimated 49 mg lung delivered dose. To allow calculation of pulmonary bioavailability and inform compartmental modelling, the plasma concentration-time profile was also evaluated after a one hour, 420 mg pirfenidone IV infusion. The duration of inhaled pirfenidone delivery to sheep (approximately 0.5 ml/min) was slightly slower when compared to inhaled delivery to naturally breathing humans (approximately 0.5 to 0.7 ml/min) (8). Despite this, the maximum sheep plasma concentration (receiving a 49 mg inhaled lung dose) was approximately two-fold higher than that in humans (receiving a 42 mg inhaled lung dose) (8). Interestingly, the plasma terminal half-life was also three-fold lower in sheep compared to humans. This suggests that some differences exist in the pulmonary pharmacokinetics of pirfenidone between the species.

One of the intended goals of this study was to use lung lymph sampling as a surrogate measure of lung interstitial pirfenidone concentrations after drug passage from the lung air spaces into the vascularised interstitium (15,16). The assumption employed was that high early interstitial concentrations would give higher drug concentrations in lung lymph than in plasma initially, but that lymph/plasma concentrations would be more similar at later times after complete absorption from the lungs. However, it was found that plasma and lymph concentrations were similar throughout much of the profile, although lymph concentrations tended to be lower than plasma during dosing, but higher at later times (beyond 3 h). This suggested that inhaled pirfenidone was absorbed from the interstitium via the blood more rapidly than the drug could equilibrate between lung interstitial fluid and lung lymph. This likely led to the rapid establishment of an equilibrium between plasma, peripheral water and the lymph via lymphatic redistribution from the blood to give the observed lymph:plasma ratio of approximately 1 after completion of dosing (17). This may be explained by the approximately 100-fold more rapid flow of blood compared to lymph (18) and the anatomy of the lung lymphatics (19–21). Specifically, absorptive alveolar regions contain limited lymphatic collecting structures when compared to around the airways and pleura. In contrast, the alveoli contain a dense vasculature that promotes the rapid absorption and lung clearance of inhaled small molecule drugs. This further suggests that lung lymph sampling is not a reliable indicator of lung interstitial drug concentrations after inhaled administration, but this is unlikely to be a problem after oral or intravenous dosing because drug concentrations in plasma will equilibrate over time with whole body interstitial fluid and lymph.

Furthermore, while the plasma concentration-time profiles suggested 2-compartment disposition kinetics, the lymph concentration-time profiles showed a pronounced 3-compartment profile in most sheep. This suggested that a pirfenidone 'reservoir' was present in sheep (likely in the lungs) that fed the continual lymphatic disposition of the drug at later time points (after the drug had been largely cleared from plasma). The identity of this reservoir was not established, however it may be residual drug located in the airways or a lung-resident cell compartment that feeds drug into the lymph at later times. Because later lymph:plasma values were greater than 2, it is unlikely that the prolonged lymphatic exposure was due to a peripheral (extra pulmonary) source of drug.

Interestingly, compared to normal healthy control subjects, lymphatic remodelling has been observed in the lungs of patients with IPF and idiopathic pulmonary pneumonia and is believed to be a key aspect of disease pathogenesis. Specifically, lymphangiogenesis involving CD11b + macrophages, together with increased lymphatic diameter and length, have been observed in the alveoli of patients with IPF (22) or idiopathic pulmonary pneumonia (23), particularly around alveolar lesions. In contrast, lymph endothelial cell and lymph vessel damage have been observed in subpleural and interlobular lymphatics in IPF patients when compared to healthy control subjects (24). Of significance to our finding of a lung lymphatic pirfenidone 'reservoir' in sheep, Khoo and colleagues showed that while plasma AUC and bioavailability remained constant, the plasma pirfenidone Cmax decreased and elimination half-life increased in IPF patients compared to healthy controls (8). While not conclusive, this data alludes to this lymphatic reservoir being important in prolonging pirfenidone clearance from human IPF lungs and may serve to enhance overall drug efficacy after inhaled administration.

High variability was noted in measured ELF pirfenidone concentrations, especially at early time points – a common observation in sheep and human ELF pharmacokinetic studies (8,25,26). For example, a study by Boisson et al. (26) reported an at least 100-fold range in ELF concentrations of colistin methanesulfonate following inhaled delivery. Regardless, ELF data were well described by the most parsimonious model incorporating rapid first order distribution from ELF into the systemic circulation (supporting information, Fig. S1). Based on the model fits to the individual sheep profiles, the average pirfenidone ELF AUC and Cmax (at the completion of dosing in each sheep) were 21.4 ± 4.6 mg·h/L and 62.3 ± 22.9 mg/L respectively, considerably higher than exposure levels in plasma.

To predict ELF Cmax over a shorter inhaled delivery time (similar to that seen in humans), ELF concentrations in 1000 virtual sheep were simulated to predict profiles over an 11 min administration time (see supporting information). From this, the Monte Carlo simulations suggested an average sheep ELF Cmax of approximately 70 mg/L (using all five sheep) and 103 mg/L (after removal of one sheep that showed a particularly low ELF:plasma ratio). In the human study (8), a single BALF sample was collected in each subject approximately 45 min after inhaled administration and ELF Cmax (occurring immediate post-inhaled dose) was predicted via extrapolation. Since the human ELF data most closely overlapped with the model that excluded one sheep, this simulation data may most accurately describe pirfenidone kinetics in humans (8). In line with the intended therapeutic goal, these results indicate ELF exposure was considerably higher than systemic exposure when pirfenidone was delivered via inhalation.

CONCLUSION

In conclusion, lung delivery of a 49 mg pirfenidone dose to sheep was well tolerated with no observed changes to lung function and respiratory dynamics. Pharmacokinetic analysis showed that ELF exposure is considerably higher after inhaled administration when compared to plasma exposure, with maximum concentrations well in excess of pirfenidone's apparent IC_{50}. Further, maximum plasma concentrations following inhaled administration were significantly lower than those obtained after oral delivery of the existing Esbriet® formulation (6). Interestingly, compartmental pharmacokinetic analysis of the data suggested the presence of a novel pirfenidone 'reservoir' that feeds lung lymphatic concentrations at times beyond those at which plasma concentrations fall below the limit of quantification. At this point, the source of this reservoir and whether it confers an inhaled therapeutic advantage for pirfenidone against IPF is unknown.

ACKNOWLEDGMENTS AND DISCLOSURES

This study was funded by Avalyn Pharma Inc. LMK is supported by an NHMRC CDF2.

REFERENCES

1. American Thoracic Society. Idiopathic pulmonary fibrosis: diagnosis and treatment. International consensus statement. American Thoracic Society (ATS), and the European Respiratory Society (ERS). Am J Respir Crit Care Med. 2000;161(2 Pt 1):646–64.
2. Spagnolo P, Del Giovane C, Luppi F, Cerri S, Balduzzi S, Walters EH, D'Amico R, Richeldi L. Non-steroid agents for idiopathic pulmonary fibrosis. Cochrane Database Syst Rev. 2010;9:CD003134.
3. Sakai N, Tager AM. Fibrosis of two: epithelial cell-fibroblast interactions in pulmonary fibrosis. Biochim Biophys Acta. 2013;1832(7):911–21.
4. Schaefer CJ, Ruhrmund DW, Pan L, Seiwert SD, Kossen K. Antifibrotic activities of pirfenidone in animal models. Eur Respir Rev. 2011;20(120):85–97.
5. Committee for Medicinal Products Human Use. CHMP assessment report. Esbret. 2010. Procedure No EMEA/H/C/002154.
6. Rubino CM, Bhavnani SM, Ambrose PG, Forrest A, Loutit JS. Effect of food and antacids on the pharmacokinetics of pirfenidone in older healthy adults. Pulm Pharmacol Ther. 2009;22(4):279–85.
7. Surber MW, Poulin D, McInally K, Chapdelaine J, Gendron D, Tat V, Murphy J, Ayaub E, Kolb MRJ, Ask K. Inhaled Pirfenidone improves animal efficacy through superior pulmonary and vascular pharmacokinetics. Am J Resp Crit Care. 2014;189
8. Khoo JK, Montgomery AB, Otto KL, Surber M, Faggian J, Lickliter JD, Glaspole I. A randomized, double-blinded, placebo-controlled, dose-escalation phase 1 study of aerosolized Pirfenidone delivered via the PARI investigational eFlow nebulizer in volunteers and patients with idiopathic pulmonary fibrosis. J Aerosol Med Pulm Drug Deliv. 2019;
9. Ryan GM, Bischof RJ, Enkhbaatar P, McLeod VM, Chan LJ, Jones SA, Owen DJ, Porter CJ, Kaminskas LM. A comparison of the pharmacokinetics and pulmonary lymphatic exposure of a generation 4 PEGylated Dendrimer following intravenous and aerosol administration to rats and sheep. Pharm Res. 2016;33(2):510–25.
10. Staub NC, Bland RD, Brigham KL, Demling R, Erdmann AJ 3rd, Woolverton WC. Preparation of chronic lung lymph fistulas in sheep. J Surg Res. 1975;19(5):315–20.
11. Rennard SI, Basset G, Lecossier D, O'Donnell KM, Pinkston P, Martin PG, Crystal RG. Estimation of volume of epithelial lining fluid recovered by lavage using urea as marker of dilution. J Appl Physiol (1985). 1986;60(2):532–8.
12. Meeusen EN, Snibson KJ, Hirst SJ, Bischof RJ. Sheep as a model for the study and treatment of human asthma and other respiratory diseases. Drug Discov Today Dis Model. 2010;6:101–6.
13. Bulitta JB, Bingolbali A, Shin BS, Landersdorfer CB. Development of a new pre- and post-processing tool (SADAPT-TRAN) for nonlinear mixed-effects modeling in S-ADAPT. AAPS J. 2011;13(2):201–11.
14. Bulitta JB, Landersdorfer CB. Performance and robustness of the Monte Carlo importance sampling algorithm using parallelized S-ADAPT for basic and complex mechanistic models. AAPS J. 2011;13(2):212–26.
15. Acred P, Brown DM, Clark BF, Mizen L. The distribution of antibacterial agents between plasma and lymph in the dog. Br J Pharmacol. 1970;39(2):439–46.

16. Anderson KE, Dencker H, Mardh PA, Akerlund M. Relationships between the concentrations of doxycycline in serum and in thoracic duct lymph after oral and intravenous administration in man. Chemotherapy. 1976;22(5):277–85.
17. Kaminskas LM, Kota J, McLeod VM, Kelly BD, Karellas P, Porter CJ. PEGylation of polylysine dendrimers improves absorption and lymphatic targeting following SC administration in rats. J Control Release. 2009;140(2):108–16.
18. Trevaskis NL, Kaminskas LM, Porter CJ. From sewer to saviour - targeting the lymphatic system to promote drug exposure and activity. Nat Rev Drug Discov. 2015;14(11):781–803.
19. Patton JS, Fishburn CS, Weers JG. The lungs as a portal of entry for systemic drug delivery. Proc Am Thorac Soc. 2004;1(4):338–44.
20. Kambouchner M, Bernaudin JF. Intralobular pulmonary lymphatic distribution in normal human lung using D2-40 antipodoplanin immunostaining. J Histochem Cytochem. 2009;57(7):643–8.
21. Schraufnagel DE. Lung lymphatic anatomy and correlates. Pathophysiology. 2010;17(4):337–43.
22. El-Chemaly S, Malide D, Zudaire E, Ikeda Y, Weinberg BA, Pacheco-Rodriguez G, Rosas IO, Aparicio M, Ren P, MacDonald SD, Wu HP, Nathan SD, Cuttitta F, McCoy JP, Gochuico BR, Moss J. Abnormal lymphangiogenesis in idiopathic pulmonary fibrosis with insights into cellular and molecular mechanisms. Proc Natl Acad Sci U S A. 2009;106(10):3958–63.
23. Lara AR, Cosgrove GP, Janssen WJ, Huie TJ, Burnham EL, Heinz DE, Curran-Everett D, Sahin H, Schwarz MI, Cool CD, Groshong SD, Geraci MW, Tuder RM, Hyde DM, Henson PM. Increased lymphatic vessel length is associated with the fibroblast reticulum and disease severity in usual interstitial pneumonia and nonspecific interstitial pneumonia. Chest. 2012;142(6):1569–76.
24. Ebina M, Shibata N, Ohta H, Hisata S, Tamada T, Ono M, Okaya K, Kondo T, Nukiwa T. The disappearance of subpleural and interlobular lymphatics in idiopathic pulmonary fibrosis. Lymphat Res Biol. 2010;8(4):199–207.
25. Landersdorfer CB, Nguyen TH, Lieu LT, Nguyen G, Bischof RJ, Meeusen EN, Li J, Nation RL, McIntosh MP. Substantial Targeting Advantage Achieved by Pulmonary Administration of Colistin Methanesulfonate in a Large-Animal Model. Antimicrob Agents Chemother. 2017;61(1)
26. Boisson M, Jacobs M, Gregoire N, Gobin P, Marchand S, Couet W, Mimoz O. Comparison of intrapulmonary and systemic pharmacokinetics of colistin methanesulfonate (CMS) and colistin after aerosol delivery and intravenous administration of CMS in critically ill patients. Antimicrob Agents Chemother. 2014;58(12):7331–9.